Approximations to wave energy absorption by articulated rafts

I.F. Noad[1] and R. Porter

School of Mathematics, University Walk, Bristol, BS8 1TW, UK

Abstract

In recent work by the authors [9] the problem of absorption of ocean wave energy by a floating articulated raft was studied. Numerical computations were shown to be rapid under a wide range of configurations but became increasingly expensive in certain limits. These included rafts either wide or narrow with respect to the incident wave direction and rafts with many articulations. The current paper proposes approximations to each of these cases resulting in a significant reduction in the numerical effort required. Typical computations are more than $40\times$ faster in the case of the wide or narrow raft approximations and it is shown that a simplified continuum model for an articulated raft predicts power absorption with less than a 1% error for rafts with 3 or more articulations.

1. Introduction

In the recent work of [9] a semi-analytic approach is developed for an articulated floating raft wave energy converter similar to that proposed by Cockerell in [3]. This consists of N buoyant pontoons connected in series via hinges so that the differential rotation of neighbouring pontoons allows energy to be extracted. The solution method developed in [9] is fully three-dimensional, the geometry of the raft being exploited to apply Fourier transforms in the plane of the free surface, where the device is situated. This approach leads to a set of $N + 2$ integral equations associated with decomposition into a set of generalised modes of motion and formulated in terms of two-dimensional unknown functions describing the hydrodynamic pressure on the underside of the raft. Approximate solutions are sought by expanding the unknowns in finite separation series of prescribed functions across both width and length of the raft. The resulting numerical calculations are very efficient for many physical parameters. However, they become increasingly expensive in the regimes shown in figure 1 and the purpose of the present paper is to develop accurate approximations to improve efficiency in these regimes.

When the raft becomes either wide or narrow relative to the incident wave direction then increasingly many terms are required in the finite separation series of the unknowns to accurately describe the rapidly varying pressure field on the underside of the raft. This, amongst other factors, leads to greater numerical expense. For the purpose of wide and narrow raft approximations it is assumed that the principal wave direction is well understood and so we consider normal incidence. For wide rafts the end effects are shown to be small so that approximate solutions may be gained by considering the two-dimensional problem. The unknown pressure force is thus dependent on the lengthways direction alone to a leading order approximation. Meanwhile for long, narrow rafts the leading order solution will be constant across the width of the raft and so the widthways dependence may be integrated out explicitly. The advantage of this is two-fold. First, by reducing the dependence of unknown functions to a single dimension the numerical complexity of the problem is reduced. Second, the convergence of infinite integrals defining inverse Fourier transforms in the widthways direction has an inverse dependence on raft width. Thus, by removing the widthways dependence of the integral equations we remove this issue of slow convergence for narrow rafts. Elongated wave energy converters are also considered by Newman in [7] using a classical slender-body theory. Whilst there must be some relation to the use of

---

[1]Corresponding author. Tel.:+44 7892 829 177.
Email addresses: imogen.noad@bristol.ac.uk (I.F. Noad), richard.porter@bristol.ac.uk (R. Porter).

two-dimensional model   full model   slender-body model

$0 \leftarrow a/b$ $Kb \rightarrow 0$

N
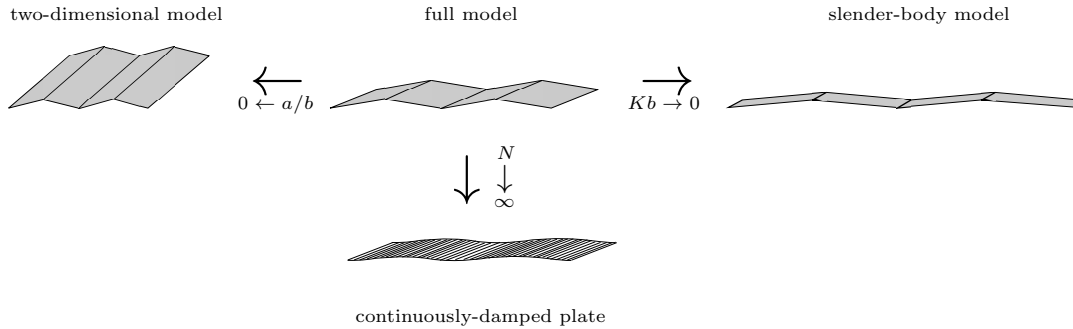$\downarrow$
∞

continuously-damped plate

Figure 1: The full model along with the three approximations for which solutions are developed in this paper.

slender-body theory, the approach used here is quite different, being obtained directly from the full integral equations.

Another factor in the complexity of the problem is the number of pontoons (N) of which the raft is comprised. Each additional component introduces an additional degree of freedom in the raft's motion and correspondingly an additional hydrodynamic problem must be solved, the problem scaling like $O(N)$. Whilst this isn't a major concern numerically, the addition of pontoons is often associated with an increased length leading to greater numerical expense as discussed above. Here, we model an articulated raft made up of a large number of hinged pontoons using a simpler continuously-damped plate model. Thus the discrete articulation and power take-off in the hinges is replaced by a flexible raft with continuous power take-off along its length. In this way the $N + 2$ problems describing the discrete modes of motion of the articulated raft reduce to a single problem describing the motion of a continuously-damped plate. Integral equations are derived in terms of the unknown vertical displacement of the raft which is intrinsically dependent on the lengthways direction alone. Thus, the complexity of the problem is further reduced, the unknown displacement being approximated by a separation series in a single variable. The theory developed here has links to models proposed for flexible ice sheets by Balmforth and Craster in [1] and the solution of the Euler-Bernoulli beam equation [5].

In §2 the parameterisation of the problem and model assumptions are introduced, the governing equations having been previously discussed in [9]. The leading order solutions for wide and narrow rafts are then developed in §3. In both cases the approximations are derived from the full integral equations of [9]. Results are then presented, both demonstrating convergence to the full model and offering a comparison of computation times. In §4 we then look at a continuously-damped plate model for the raft, a simpler configuration which is shown to accurately model a floating raft made up of an increasing number of pontoons. A set of discrete equations of motion associated with the vertical and rotational motions of the individual pontoons is used to derive a continuous kinematic surface condition which incorporates the complete dynamics of the flexible raft. The solution for the associated hydrodynamic problem is then developed along with expressions for the power associated with a continuous power take-off mechanism. Finally, results are presented with the intention of both demonstrating convergence of the full model to the approximation and inspecting the motions of the raft. In §5 overall conclusions are drawn.

2. Formulation

In this paper we will develop approximate solutions to hydrodynamic problems describing an articulated raft wave energy converter. In the previous work of the authors [9] a solution of the full three-dimensional problem was developed. Here we are concerned with developing approximations in the three regimes shown in figure 1. We begin by outlining the problem. Cartesian coordinates are chosen with the origin in the mean free surface level and z pointing vertically upwards. The fluid has density ρ and is of infinite depth, inviscid and incompressible. Fluid motions are irrotational and of small amplitude. A hinged raft of thickness h and density
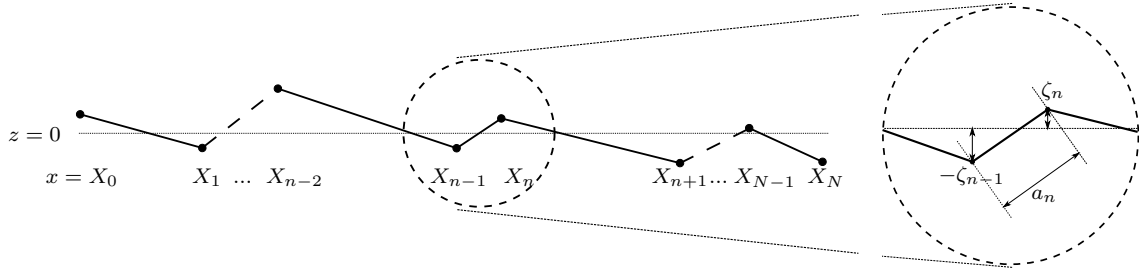
2

Figure 2: Some key parameters imposed on a side view (and close-up) of the articulated raft converter used in the hydrodynamic model.

$\rho_s < \rho$ floats on the surface of the water with shallow draft $d = \rho_s h/\rho$. It is comprised of N rectangular sections as shown in figure 2, each of width $2b$ and hinged along $x = X_n$ for $n = 1, ..., N-1$, $-b < y < b$. This definition is extended to the fore and aft ends of the raft which are located at $x = X_0$ and X_N respectively. The entire raft is centred at the origin and occupies a region

$$\mathcal{D} = \bigcup_{n=1}^{N} \mathcal{D}_n \qquad \text{with} \qquad \mathcal{D}_n = \{(x,y)|X_{n-1} < x < X_n, -b < y < b\} \qquad (2.1)$$

being the planform of the nth pontoon and $a_n = X_n - X_{n-1}$ its length. Finally, we denote the total length of the raft by $2a = (X_N - X_0)$ so that $X_0 = -a$ and $X_N = a$.

Monochromatic plane waves of radian frequency ω are incident from $x < 0$, making an anti-clockwise angle $\theta_0 \in (-\pi/2, \pi/2)$ with the positive x-direction. We shall assume waves of small steepness $KA \ll 1$ where A is the wave amplitude and $2\pi/K$ is the wavelength with $K = \omega^2/g$ being the wave number and g the gravitational acceleration. Damping devices placed along each hinge enable power take-off, exerting a force opposing and in proportion to the rate of change of angle made between adjacent plates. The vertical displacements of the hinges are denoted by $\zeta_n(t)$.

Under the assumptions made the fluid velocity is described as the gradient of a scalar velocity potential $\Phi(x, y, z, t)$ satisfying the hydrodynamic problem stated in [9, (2.3-2.6)].

3. Articulated raft approximations

In the case of the wide and narrow articulated raft approximations it is convenient use the principle of linear superposition to decompose the velocity potential and factor out harmonic time dependence, writing

$$\Phi(x, y, z, t) = \Re \left\{ \left((-iAg/\omega)\, \phi_S(x, y, z) + \sum_{n=0}^{N} U_n \phi_n(x, y, z) \right) e^{-i\omega t} \right\} \qquad (3.1)$$

where ϕ_S describes the waves scattered by a fixed horizontal raft, satisfying

$$\frac{\partial \phi_S}{\partial z}(x, y, 0) = 0 \qquad \text{for } (x, y) \in \mathcal{D} \qquad (3.2)$$

along with [9, (2.8-2.10)], whilst the second term in (3.1) describes a decomposition into a set of generalised modes of motion outlined in [9, §3]. Thus, the coefficients U_n describe generalised velocities whilst the functions $\phi_n(x, y, z)$ describe radiation potentials associated with forced oscillatory motion in each of the generalised modes, satisfying

$$\frac{\partial \phi_n}{\partial z}(x, y, 0) = f_n(x) \qquad \text{for } (x, y) \in \mathcal{D} \qquad (3.3)$$

3

along with [9, (2.8-2.10)], for $n = 0, ..., N$. Here $f_n(x)$ are prescribed functions forming a basis for the plate motion and are defined in [9, §3]. They provide the forcing in the hydrodynamic problems associated with the radiation of waves. Meanwhile, the forcing in the scattering problem is provided by the incident wave

$$\phi_I(x, y, z) = e^{i\alpha_0 x} e^{i\beta_0 y} e^{Kz}, \tag{3.4}$$

where $\alpha_0 = K \cos\theta_0$ and $\beta_0 = K \sin\theta_0$. Finally, the potentials $\phi_S - \phi_I$ and ϕ_n describe outgoing waves at large distances from the raft.

In [9, §5] integral equations are derived for the unknown functions $\phi_{S,n}(x, y, 0)$. The unknown functions are evaluated at $z = 0$ and represemt the pressure force on the underside of the raft. Thus, we have

$$\phi_{S,n}(x, y, 0) + (\mathcal{K}\phi_{S,n})(x, y, 0) = D_{S,n}(x, y) \qquad \text{for } (x, y) \in \mathcal{D} \text{ and } n = 0, ..., N \tag{3.5}$$

where

$$(\mathcal{K}\phi)(x, y, 0) = \frac{1}{4\pi^2} \int_{-\infty}^{\infty} \int_{-\infty}^{\infty} \frac{K}{k - K} \iint_{\mathcal{D}} \phi(x', y', 0) e^{-i\alpha x'} e^{-i\beta y'} \, dx' \, dy' \, e^{i\alpha x} e^{i\beta y} \, d\alpha \, d\beta \tag{3.6}$$

with $k = \sqrt{\alpha^2 + \beta^2}$. Here the forcing associated with the scattering problem is given by

$$D_S(x, y) = e^{i\alpha_0 x} e^{i\beta_0 y} \tag{3.7}$$

whilst the forcing associated with the radiation problems is given by

$$D_n(x, y) = \frac{1}{4\pi^2} \int_{-\infty}^{\infty} \int_{-\infty}^{\infty} \frac{1}{k - K} \iint_{\mathcal{D}} f_n(x') e^{-i\alpha x'} e^{-i\beta y'} \, dx' \, dy' \, e^{i\alpha x} e^{i\beta y} \, d\alpha \, d\beta \tag{3.8}$$

for $n = 0, ..., N$.

3.1. Approximation for a wide raft

With the prominent incident wave direction aligned close to the positive x-axis so that θ_0 is assumed small we set out to approximate the solution of the integral equations (3.5) for a wide raft, that is $Kb \gg 1$, $Ka = O(1)$ and $b/a \gg 1$. We begin by considering the scattering problem. If the raft is wide we expect the solution to be dominated by a component which represents the scattering by a raft of infinite width. Thus, we write

$$\phi_S(x, y, 0) \simeq \psi_S(x) e^{i\beta_0 y} + R_S(x, y) \tag{3.9}$$

in which the first term encodes the decomposition one would have used in a two-dimensional scattering problem whilst $R_S(x, y)$ is envisaged as a 'correction' due to end effects. Substituting for (3.9) in (3.5) then gives

$$\psi_S(x) e^{i\beta_0 y} + \frac{K}{2\pi i} \int_{-\infty}^{\infty} \left[e^{i\beta_0 b} I(\alpha, y - b; \beta_0) - e^{-i\beta_0 b} I(\alpha, y + b; \beta_0) \right] \int_{-a}^{a} \psi_S(x') e^{-i\alpha x'} \, dx' e^{i\alpha x} \, d\alpha$$
$$+ R_S(x, y) + (\mathcal{K}R_S)(x, y) = D_S(x, y) \tag{3.10}$$

where

$$I(\alpha, y; \beta_0) = \frac{1}{2\pi} \int_{-\infty}^{\infty} \frac{e^{i\beta y}}{\left(\sqrt{\alpha^2 + \beta^2} - K\right)(\beta_0 - \beta)} \, d\beta. \tag{3.11}$$

We evaluate the integral defined in (3.11) by assigning a small positive imaginary part to the frequency ω which is eventually set to zero. This manifests itself by moving the poles at $\beta = \pm\sqrt{K^2 - \alpha^2}$ above and below the real β-axis respectively. The contour is then deformed into the upper and lower-half β-plane for $y > 0$ and $y < 0$ respectively, with deformations around the

4

branch cuts on the imaginary axis for $|\Im\{\beta\}| > |\alpha|$ and above the pole on the real-axis at $\beta = \beta_0$. This results in

$$I(\alpha, y; \beta_0) = -\frac{i}{2}\operatorname{sgn}(y)\frac{e^{i\beta_0 y}}{\sqrt{\alpha^2 + \beta_0^2 - K}} + \frac{Ke^{-\lambda(\alpha, K)|y|}}{\lambda(\alpha, K)\left(\beta_0 - i\operatorname{sgn}(y)\lambda(\alpha, K)\right)}$$
$$+ \frac{1}{\pi}\int_{|\alpha|}^{\infty}\frac{\sqrt{s^2 - \alpha^2}e^{-s|y|}}{\left(s^2 - \alpha^2 + K^2\right)\left(\beta_0 - i\operatorname{sgn}(y)s\right)}\,ds \tag{3.12}$$

where

$$\lambda(\alpha, K) = \sqrt{\alpha^2 - K^2} \qquad = -i\sqrt{K^2 - \alpha^2} \qquad \text{when } |\alpha| < K \tag{3.13}$$

with the choice of branch being chosen to ensure the radiation condition is satisfied. Substituting for (3.12) in (3.10) we then gain

$$\left[\psi_S(x) + \frac{K}{2\pi}\int_{-\infty}^{\infty}\frac{e^{i\alpha x}}{\sqrt{\alpha^2 + \beta_0^2 - K}}\int_{-a}^{a}\psi_S(x')e^{-i\alpha x'}\,dx'\,d\alpha\right]e^{i\beta_0 y} + R_S(x, y) + (\mathcal{K}R_S)(x, y)$$
$$= D_S(x, y) + e^{-i\beta_0 b}\left(\left[\mathcal{G} + \mathcal{H}\right]\psi_S\right)(x, y + b; \beta_0) - e^{i\beta_0 b}\left(\left[\mathcal{G} + \mathcal{H}\right]\psi_S\right)(x, y - b; \beta_0) \tag{3.14}$$

where the integral operators $\mathcal{G}$ and $\mathcal{H}$ are defined by

$$(\mathcal{G}\psi)(x, y; \beta_0) = \frac{K}{2\pi i}\int_{-\infty}^{\infty}\frac{Ke^{i\alpha x}e^{-\lambda(\alpha, K)|y|}}{\lambda(\alpha, K)\left(\beta_0 - i\operatorname{sgn}(y)\lambda(\alpha, K)\right)}\int_{-a}^{a}\psi(x')e^{-i\alpha x'}\,dx'\,d\alpha \tag{3.15}$$

and

$$(\mathcal{H}\psi)(x, y; \beta_0) = \frac{K}{2\pi^2 i}\int_{-\infty}^{\infty}e^{i\alpha x}\int_{|\alpha|}^{\infty}\frac{\sqrt{s^2 - \alpha^2}e^{-s|y|}}{\left(s^2 - \alpha^2 + K^2\right)\left(\beta_0 - i\operatorname{sgn}(y)s\right)}\,ds\int_{-a}^{a}\psi(x')e^{-i\alpha x'}\,dx'\,d\alpha. \tag{3.16}$$

Since $\psi_S(x)$ is the solution to the two-dimensional problem, satisfying the same integral equation as the two-dimensional plate considered in [10],

$$\psi_S(x) + \frac{K}{2\pi}\int_{-\infty}^{\infty}\frac{e^{i\alpha x}}{\sqrt{\alpha^2 + \beta_0^2 - K}}\int_{-a}^{a}\psi_S(x')e^{-i\alpha x'}\,dx'\,d\alpha = e^{i\alpha_0 x}, \tag{3.17}$$

then the corresponding terms may be cancelled in (3.14) to leave an integral equation for the unknown correction

$$R_S(x, y) + (\mathcal{K}R_S)(x, y) = e^{-i\beta_0 b}\left(\left[\mathcal{G} + \mathcal{H}\right]\psi_S\right)(x, y + b; \beta_0) - e^{i\beta_0 b}\left(\left[\mathcal{G} + \mathcal{H}\right]\psi_S\right)(x, y - b; \beta_0) \tag{3.18}$$

for $(x, y) \in \mathcal{D}$. Here the forcing terms are located at the widthways end-points of the raft, $y = \pm b$, the correction $R_S(x, y)$ describing the end effects. Using Watson's Lemma it may be shown that

$$\left(\left[\mathcal{G} + \mathcal{H}\right]\psi\right)(x, y; \beta_0) \sim -\frac{e^{iK|y|}}{\sqrt{|y|}}\frac{\sqrt{K^3/8\pi}}{\beta_0 - \operatorname{sgn}(y)K}\int_{-a}^{a}\psi(x')dx' \tag{3.19}$$

as $|y| \to \infty$, the forcing due to end effects decaying away from the end-points. We decompose $R_S(x, y)$ so that

$$R_S(x, y) = e^{-i\beta_0 b}C_S(x, y + b) - e^{i\beta_0 b}C_S(x, y - b) \tag{3.20}$$

where

$$C_S(x, y) + (\mathcal{K}C_S)(x, y) = \left(\left[\mathcal{G} + \mathcal{H}\right]\psi_S\right)(x, y; \beta_0), \tag{3.21}$$

5

and $C_S(x, y \pm b)$ describes the response to forcing located at each of the end-points. If we substitute for

$$C_S(x, y) = C \operatorname{sgn}(y) \frac{e^{iK|y|}}{\sqrt{|y|}} \qquad (3.22)$$

for a complex constant C then it may be shown for $\beta_0 = 0$ that

$$C_S(x, y) + (\mathcal{K}C_S)(x, y) \sim \operatorname{sgn}(y) \frac{e^{iK|y|}}{\sqrt{|y|}} C \left(iKa \left(2\sqrt{2/\pi} + 1 \right) + 1 \right) \qquad (3.23)$$

as $|y| \to \infty$ and $b \to \infty$. So, for a wide raft the leading order behaviour of $C_S(x, y)$ is localised at the end-points. No further analytic progress has been made beyond (3.21) to, for example, find bounds on the effect of $C_S(x, y)$ on properties of the solution such as the forces that contribute to raft motion. One could solve (3.21) numerically using techniques in [9] but this would not provide any improvement to numerical efficiency.

In the case of the N modes associated with the radiation of waves then we expect the solution to be dominated by a component which represents the radiation of waves by a raft of infinite width. Thus, we write

$$\phi_n(x, y, 0) \simeq \psi_n(x) + R_n(x, y) \qquad \text{for } n = 0, ..., N \qquad (3.24)$$

where $\psi_n(x)$ satisfies the two-dimensional problem

$$\psi_n(x) + \frac{K}{2\pi} \int_{-\infty}^{\infty} \frac{e^{i\alpha x}}{|\alpha| - K} \int_{-a}^{a} \psi_n(x') e^{-i\alpha x'} dx' d\alpha = \frac{1}{2\pi} \int_{-\infty}^{\infty} \frac{e^{i\alpha x}}{|\alpha| - K} \int_{-a}^{a} f_n(x') e^{-i\alpha x'} dx' d\alpha, \qquad (3.25)$$

for $x \in (-a, a)$ and $R_n(x, y)$ is a correction due to the end effects. In the case of the radiation problem then $D_n(x, y)$ may also be expressed in terms of the integral $I(\alpha, y; \beta_0)$, giving

$$D_n(x, y) = \frac{i}{2\pi} \int_{-\infty}^{\infty} [I(\alpha, y + b; 0) - I(\alpha, y - b; 0)] \int_{-a}^{a} f_n(x') e^{-i\alpha x'} dx' \, e^{i\alpha x} d\alpha \qquad (3.26)$$

$$= \frac{1}{2\pi} \int_{-\infty}^{\infty} \frac{1}{|\alpha| - K} \int_{-a}^{a} f_n(x') e^{-i\alpha x'} dx' \, e^{i\alpha x} d\alpha$$
$$+ ([\mathcal{G} + \mathcal{H}] f_n)(x, y + b; 0) - ([\mathcal{G} + \mathcal{H}] f_n)(x, y - b; 0) \qquad (3.27)$$

where the integral operators $\mathcal{G}$ and $\mathcal{H}$ were defined earlier in (3.15) and (3.16). Substituting for the decomposition (3.24) in the integral equation (3.5), using (3.27) and (3.12) and cancelling terms associated with the two-dimensional problem we ultimately gain an integral equation for the unknown corrections

$$R_n(x, y) + (\mathcal{K}R_n)(x, y) = ([\mathcal{G} + \mathcal{H}](\psi_n + f_n))(x, y + b; 0) - ([\mathcal{G} + \mathcal{H}](\psi_n + f_n))(x, y - b; 0) \qquad (3.28)$$

for $n = 0, ..., N$. As with the scattering problem the forcing due to end effects decays away from the end-points and so $R_n(x, y)$ will be localised for $n = 0, ..., N$. Making an analogous decomposition to (3.20)

$$R_n(x, y) = e^{-i\beta_0 b} C_n(x, y + b) - e^{i\beta_0 b} C_n(x, y - b) \qquad (3.29)$$

where

$$C_n(x, y) + (\mathcal{K}C_n)(x, y) = ([\mathcal{G} + \mathcal{H}](\psi_n + f_n))(x, y; 0) \qquad (3.30)$$

for $n = 0, ..., N$ then the leading order behaviour for a wide raft is localised at the end-points $C_n(x, y)$.

6

Combining the solutions to the scattering and radiation problems we may now determine the force per unit width exerted on the raft in the nth mode. This is given by

$$\frac{F_n}{2b} = \frac{i\omega\rho}{2b} \iint_{\mathcal{D}} \left(\frac{-iAg}{\omega}\phi_S(x,y,0) + \sum_{m=0}^{N} U_m\phi_m(x,y,0) \right) f_n(x)\, dS \tag{3.31}$$

$$= \frac{i\omega\rho}{2b} \iint_{\mathcal{D}} \left(\frac{-iAg}{\omega}\psi_S(x) + \sum_{m=0}^{N} U_m\psi_m(x) \right) f_n(x)\, dS$$

$$+ \int_{-a}^{a} \left[\frac{\rho g A}{b} \int_0^{2b} C_S(x,y)\, dy + \frac{i\omega\rho}{b} \sum_{m=0}^{N} \int_0^{2b} C_m(x,y)\, dy \right] f_n(x)\, dx$$

$$\xrightarrow{b\to\infty} i\omega\rho \int_{-a}^{a} \left(\frac{-iAg}{\omega}\psi_S(x) + \sum_{m=0}^{N} U_m\psi_m(x) \right) f_n(x)\, dx \tag{3.32}$$

for $n = 0,...,N$ where the last line results since

$$\int_0^{2b} C_{S,n}(x,y)\, dy \xrightarrow{b\to\infty} \int_0^{\infty} C_{S,n}(x,y)\, dy, \tag{3.33}$$

leading to a convergent integral which is independent of b. Thus, for wide rafts the force per unit width is well approximated by the force per unit width exerted on a raft of infinite extent and so the power take-off from a wide raft may be approximated by the two-dimensional problem. This decomposition of the problem for a wide raft into a two-dimensional problem along with corrections which encode the end-effects from a semi-infinite geometry is similar to the decomposition pursued in [11] for long finite arrays.

Next, we solve (3.17) and (3.25) for ψ_S and ψ_n for $n = 0,...,N$. The radiation condition dictates that

$$\psi_S(x) \sim \begin{cases} e^{iKx} + Re^{-iKx} & x \to -\infty \\ Te^{iKx} & x \to \infty \end{cases} \tag{3.34}$$

where R and T are the complex radiation and transmission coefficients, given by

$$R = -iK \int_{-a}^{a} \psi_S(x)e^{iKx}\, dx \qquad \text{and} \qquad T = 1 - iK \int_{-a}^{a} \psi_S(x)e^{-iKx}\, dx. \tag{3.35}$$

This describes the amplitudes of the outgoing waves in the farfield in terms of the unknown potential ψ_S. Meanwhile

$$\psi_n(x) \sim aA_n^{\pm}e^{\pm iKx} \qquad x \to \pm\infty. \tag{3.36}$$

where the radiated wave amplitudes are given by

$$aA_n^{\pm} = i \int_{-a}^{a} \left(f_n(x') - K\psi_n(x') \right) e^{\mp iKx'}\, dx'. \tag{3.37}$$

To solve (3.17) and (3.25) we employ a Galerkin expansion method, expanding the unknown functions in terms of a complete set of orthogonal functions

$$\psi_S(x) = \sum_{p=0}^{\infty} c_p^S v_p\left(\frac{x}{a}\right) \qquad \text{and} \qquad \psi_n(x) = 2a \sum_{p=0}^{\infty} c_p^{(n)} v_p\left(\frac{x}{a}\right), \tag{3.38}$$

where $v_r(t) = \frac{1}{2}e^{ir\pi/2}P_r(t)$ and $P_r(t)$ are orthogonal Legendre polynomials satisfying

$$\int_{-1}^{1} P_r(t)P_s(t)\, dt = \frac{2\delta_{rs}}{2r+1} \qquad \text{and} \qquad \int_{-1}^{1} P_r(t)e^{-i\sigma t}\, dt = 2e^{-ir\pi/2}j_r(\sigma), \tag{3.39}$$

7

as in [10] where $j_r(\sigma)$ denote spherical Bessel functions. Multiplying (3.17) through by $v_q^*(x/a)/a$ and (3.25) by $v_q^*(x/a)/2a^2$ then integrating over $x \in (-a, a)$ we gain the following systems of equations for the unknown coefficients

$$\frac{c_q^S}{2(2q+1)} + \sum_{p=0}^{\infty} c_p^S K_{pq}(\beta_0) = j_q(Ka) \qquad \text{for } q = 0, 1, 2, \ldots \qquad (3.40)$$

and

$$\frac{c_q^{(n)}}{2(2q+1)} + \sum_{p=0}^{\infty} c_p^{(n)} K_{pq}(0) = \frac{Ka}{2\pi} \int_{-\infty}^{\infty} \frac{j_q(\alpha a)}{|\alpha| - K} \frac{1}{2Ka^2} \int_{-a}^{a} f_n(x') e^{-i\alpha x'} \, dx' \, d\alpha \qquad (3.41)$$

for $q = 0, 1, 2, \ldots$ and $n = 0, \ldots, N$ where

$$K_{pq}(\beta_0) = \frac{Ka}{2\pi} \int_{-\infty}^{\infty} \frac{j_p(\alpha a) j_q(\alpha a)}{\sqrt{\alpha^2 + \beta_0^2} - K} \, d\alpha \qquad \text{for } p, q = 0, 1, 2, \ldots \qquad (3.42)$$

Indenting around the poles at $\alpha = \pm\sqrt{K^2 - \beta_0^2}$ and noting that the integral vanishes unless $p + q$ is even we may write

$$K_{2p+\nu, 2q+\nu}(\beta_0) = iKa \frac{j_{2p+\nu}(Ka) j_{2q+\nu}(Ka)}{\cos\theta_0} + \frac{Ka}{\pi} \int_0^{\infty} \frac{j_{2p+\nu}(\alpha a) j_{2q+\nu}(\alpha a)}{\sqrt{\alpha^2 + \beta_0^2} - K} \, d\alpha \qquad (3.43)$$

for $p, q = 0, 1, 2, \ldots$ and $\nu = 0, 1$ resulting in a decoupling of (3.40) and (3.41) into symmetric and antisymmetric parts. If we expand the generalised modes in terms of the same set of basis functions as used in (3.38),

$$f_n(x) = \sum_{k=0}^{\infty} \alpha_k^{(n)} v_k\left(\frac{x}{a}\right) \qquad \text{for } n = 0, \ldots, N, \qquad (3.44)$$

then we may also express the right hand side of (3.41) in terms of the integrals $K_{pq}(0)$. Ultimately, we write

$$\frac{c_{2q+\nu}^{(n)}}{2(4q+2\nu+1)} + \sum_{p=0}^{\infty} c_{2p+\nu}^{(n)} K_{2p+\nu, 2q+\nu}(0) = \frac{1}{2Ka} \sum_{k=0}^{\infty} \alpha_{2k+\nu}^{(n)} K_{2k+\nu, 2q+\nu}(0) \qquad (3.45)$$

for $q = 0, 1, 2, \ldots$ where

$$\alpha_k^{(n)} = 2(2k+1) \int_{-1}^{1} f_n(at) v_k^*(t) \, dt \qquad \text{for } n = 0, \ldots, N. \qquad (3.46)$$

The efficiency may then be calculated using either the expression for power given in [9] or conservation of energy, which results in

$$E = 1 - |R_{total}|^2 - |T_{total}|^2 \qquad (3.47)$$

where

$$R_{total} = R + \sum_{n=0}^{N} U_n A_n^- = -iKa \sum_{p=0}^{\infty} j_p(-Ka) \left[c_p^S + 2 \sum_{n=0}^{N} U_n \left(c_p^{(n)} - \alpha_p^{(n)}/2Ka \right) \right] \qquad (3.48)$$

and

$$T_{total} = T + \sum_{n=0}^{N} U_n A_n^+ = 1 - iKa \sum_{p=0}^{\infty} j_p(Ka) \left[c_p^S + 2 \sum_{n=0}^{N} U_n \left(c_p^{(n)} - \alpha_p^{(n)}/2Ka \right) \right]. \qquad (3.49)$$

8

3.2. Approximation for a narrow raft

In this secion we consider a narrow raft aligned parallel to the positive x-axis and subject to a prominent incident wave direction θ_0 which is assumed to be small so that the incident wave field is aligned along the length of the raft. It is assumed that $Kb \ll 1$, $Ka = O(1)$ and $b/a \ll 1$. Since the raft is narrow we expect the pressure to be approximately constant across the width of the raft, that is $\phi(x, y, 0) \simeq \phi(x, 0, 0)$ for $(x, y) \in \mathcal{D}$. This allows the $y-$dependence of the integral equations (3.5) to be evaluated explicitly, an approach which differs from that used in [7] in which elongated bodies are considered using a classical slender-body theory. We begin by evaluating the integral w.r.t y' using

$$\int_{-b}^{b} e^{-i\beta y'} \, dy' \simeq 2b. \tag{3.50}$$

Then, we evaluate the inverse Fourier transform w.r.t β. This follows similarly to the evaluation of $I(\alpha, y; \beta_0)$ (defined in (3.11)) only without the pole at $\beta = \beta_0$. We assign a small positive imaginary part to the frequency ω, moving the poles at $\beta = \pm\sqrt{K^2 - \alpha^2}$ above and below the real β-axis respectively and allowing the contour of integration to run along the real β-axis. We deform the contour into the upper and lower-half β-plane for $y > 0$ and $y < 0$ respectively accounting for contributions due to the branch cuts on the imaginary axis for $|\Im\{\beta\}| > |\alpha|$. Finally, the small imaginary part of the frequency is set to zero and we find

$$\frac{1}{2\pi} \int_{-\infty}^{\infty} \frac{e^{i\beta y}}{k - K} \int_{-b}^{b} e^{-i\beta y'} \, dy' \, d\beta = 2b \left[\frac{Ke^{-\lambda(\alpha, K)|y|}}{\lambda(\alpha, K)} + \frac{\operatorname{sgn}(y)}{\pi} \int_{|\alpha|}^{\infty} \frac{e^{-|y|s}\sqrt{s^2 - \alpha^2}}{s^2 - \alpha^2 + K^2} \, ds \right] \tag{3.51}$$

where $\lambda(\alpha, K)$ was defined earlier in (3.13). Substituting (3.51) and the expansion

$$\phi_S(x, y, 0) \simeq \sum_{p=0}^{\infty} d_p^S v_p \left(\frac{x}{a} \right) \tag{3.52}$$

into (3.5), multiplying by $v_q^*(x/a)/2ab$ and integrating over $(x, y) \in \mathcal{D}$ we then gain the sets of equations

$$\frac{d_q^S}{2(2q + 1)} + 2Kb \sum_{p=0}^{\infty} d_p^S S_{pq} = j_q(\alpha_0 a) \qquad \text{for } p, q = 0, 1, 2, \ldots \tag{3.53}$$

where

$$S_{pq} = \frac{Ka}{2\pi} \int_{-\infty}^{\infty} \frac{j_p(\alpha a) j_q(\alpha a)}{\lambda(\alpha, K)} \, d\alpha. \tag{3.54}$$

We note that the integrals vanish unless $p + q$ is even in which case

$$S_{2p+\nu, 2q+\nu} = \frac{Ka}{\pi} \int_0^{\infty} \frac{j_{2p+\nu}(\alpha a) j_{2q+\nu}(\alpha a)}{\lambda(\alpha, K)} \, d\alpha \qquad \text{for } p, q = 0, 1, 2, \ldots \text{ and } \nu = 0, 1 \tag{3.55}$$

and (3.53) thus decouples into symmetric and antisymmetric parts. Expanding about $Kb = 0$ then results in approximations for our unknown coefficients

$$d_{2q+\nu}^S \simeq 2(4q + 2\nu + 1) j_{2q+\nu}(\alpha_0 a) - 8Kb \sum_{p=0}^{\infty} j_{2p+\nu}(\alpha_0 a)(4p + 2\nu + 1)(4q + 2\nu + 1) S_{2p+\nu, 2q+\nu}^{sl} \tag{3.56}$$

for $q = 0, 1, 2 \ldots$ and $\nu = 0, 1$.

The solution for the $N + 1$ modes associated with the radiation problem follows similarly. Expanding the unknown functions as

$$\phi_n(x, 0, 0) \simeq 2a \sum_{p=0}^{\infty} d_p^{(n)} v_p \left(\frac{x}{a} \right) \qquad \text{for } n = 0, \ldots, N \tag{3.57}$$

we ultimately find

$$d_{2q+\nu}^{(n)} \simeq 2(4q + 2\nu + 1)\frac{2Kb}{2Ka}\sum_{k=0}^{\infty}\alpha_{2k+\nu}^{(n)}S_{2k+\nu,2q+\nu} \quad \text{for } q = 0, 1, 2, \dots \text{ and } \nu = 0, 1 \qquad (3.58)$$

when $Kb \ll 1$ where $\alpha_k^{(n)}$ are the expansion coefficients of $f_n(x)$ defined earlier in (3.46).

3.3. Numerical Calculations and Results

The numerical integration of S_{pq} requires the integral to be rearranged since in the form shown in (3.54) the integrand is unbounded near $|\alpha| = K$. One way to overcome this issue is to make the substitution $\alpha = K\cos u$ for $\alpha < K$ and $\alpha = K\cosh u$ for $\alpha > K$. However, this leads to a rapidly oscillating integral and we instead choose to make use of the integral identities

$$\int_0^1 \frac{J_m(a\zeta)}{\sqrt{1-\zeta^2}}d\zeta = \frac{\pi}{2}\left[J_{\frac{m}{2}}\left(\frac{a}{2}\right)\right]^2 \quad \text{and} \quad \int_1^{\infty}\frac{J_m(a\zeta)}{\sqrt{\zeta^2-1}}d\zeta = -\frac{\pi}{2}J_{\frac{m}{2}}\left(\frac{a}{2}\right)Y_{\frac{m}{2}}\left(\frac{a}{2}\right) \qquad (3.59)$$

for $a > 0$ (Gradshteyn and Ryzhik [4], §6.552(4,6)) along with the relation

$$j_n(x) = \sqrt{\frac{\pi}{2x}}J_{n+\frac{1}{2}}(x). \qquad (3.60)$$

These allow us to write

$$S_{2p+\nu,2q+\nu} = \frac{Ka}{\pi}\int_0^{\infty}\frac{\left(j_{2p+\nu}(\alpha a) - \sqrt{\alpha/K}j_{2p+\nu}(Ka)\right)}{\lambda(\alpha,K)}j_{2q+\nu}(\alpha a)\,d\alpha$$
$$+ \frac{i\pi}{4}J_{2p+\nu+\frac{1}{2}}(Ka)\,J_{\frac{2q+\nu}{2}+\frac{1}{4}}\left(\frac{Ka}{2}\right)H_{\frac{2q+\nu}{2}+\frac{1}{4}}^{(1)}\left(\frac{Ka}{2}\right) \qquad (3.61)$$

for $p, q = 0, 1, 2, \dots$ and $\nu = 0, 1$ in which the integrand now vanishes as $\alpha \to K$, resolving the numerical issue. In this process we have also slowed the decay so it aids convergence to further employ another integral result (Gradshteyn and Ryzhik [4], §6.552(1)) to explicitly calculate the leading order contribution

$$\int_0^{\infty}\frac{\sqrt{\alpha/K}j_{2q+\nu}(\alpha a)}{\sqrt{\alpha^2 + K^2}}d\alpha = \sqrt{\frac{\pi}{2Ka}}I_{\frac{2q+\nu}{2}+\frac{1}{4}}\left(\frac{Ka}{2}\right)K_{\frac{2q+\nu}{2}+\frac{1}{4}}\left(\frac{Ka}{2}\right) \qquad (3.62)$$

where $I_n(t)$ and $K_n(t)$ are modified Bessel functions. Thus, for the purpose of numericl integration we use

$$S_{2p+\nu,2q+\nu} = \frac{Ka}{\pi}\int_0^{\infty}\left(\frac{\left(j_{2p+\nu}(\alpha a) - \sqrt{\alpha/K}j_{2p+\nu}(Ka)\right)}{\lambda(\alpha,K)} + \frac{\sqrt{\alpha/K}j_{2p+\nu}(Ka)}{\sqrt{\alpha^2 + K^2}}\right)j_{2q+\nu}(\alpha a)\,d\alpha$$
$$- \frac{1}{2}J_{2p+\nu+\frac{1}{2}}(Ka)I_{\frac{2q+\nu}{2}+\frac{1}{4}}\left(\frac{Ka}{2}\right)K_{\frac{2q+\nu}{2}+\frac{1}{4}}\left(\frac{Ka}{2}\right)$$
$$+ \frac{i\pi}{4}J_{2p+\nu+\frac{1}{2}}(Ka)\,J_{\frac{2q+\nu}{2}+\frac{1}{4}}\left(\frac{Ka}{2}\right)H_{\frac{2q+\nu}{2}+\frac{1}{4}}^{(1)}\left(\frac{Ka}{2}\right) \qquad (3.63)$$

for $q, p = 0, 1, 2, \dots$ and $\nu = 0, 1$ where the integrand now has cubic decay and vanishes near $|\alpha| = K$.

Infinite summations associated with the unknown functions and bending modes are truncated at $p = q = k = P$ in numerical computations and spherical Bessel functions are calculated using a Fortran routine [2].

Results will be presented in terms of the efficiency and its three-dimensional analogue, the capture factor, a dimensionless measure of power absorption defined to be the ratio of power absorbed to power available in the equivalent crest length of incident wave to the width of the device
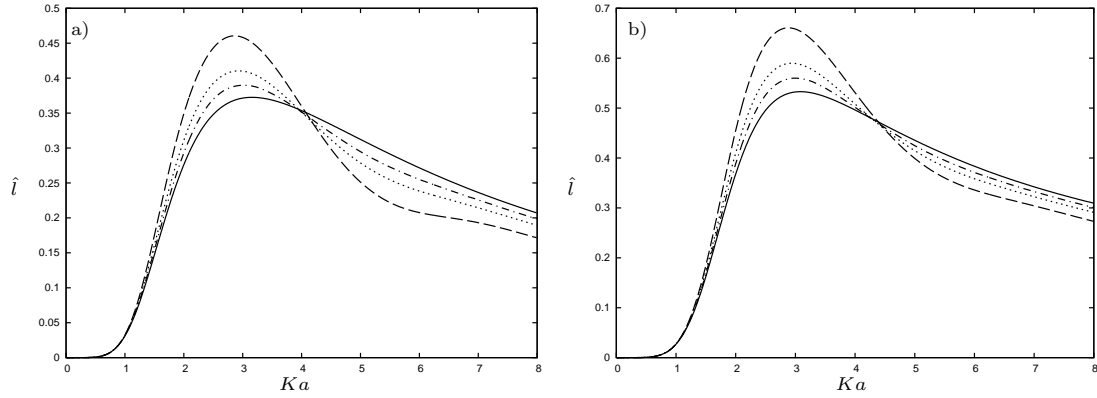
$$\hat{l} = \frac{W}{2bW_{inc}}. \qquad (3.64)$$

10

Figure 3: Figures show $\hat{l}$ as a function of Ka. In both cases two-dimensional results are shown by a solid line whilst $b/a = 1, 2, 4$ are shown by the dashed, dotted and chained lines respectively. Figures (a) and (b) show results for systems made up of 2 and 4 equally-sized pontoons respectively. In both cases $\hat{\lambda}_n = 0.01$ for all n, $s = 0.6$ and $a/h = 10$.
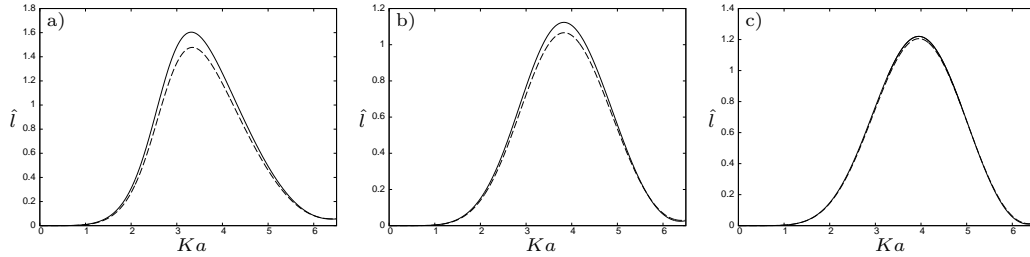

Figure 4: Figures show $\hat{l}$ as a function of Ka for two equally-sized pontoons with $d/2b = 0.5$ and $\hat{\lambda}_1 = 0.001$ fixed. Results of the full model are shown by the solid line whilst slender-body approximations are shown by the dashed lines. Figures $(a) - (c)$ show results for $Kb = 0.4, 0.2$ and 0.1 respectively, agreement improving as Kb decreases.

We also use a dimensionless form for the power take-off parameters, writing $\hat{\lambda}_n = \lambda_n / 16\rho\omega a^4 b$.

In Figure 3 the convergence of results computed using the full model of [9] to the two-dimensional approximation is demonstrated in two different instances, (a) and (b) corresponding to systems of two and four equally-sized pontoons respectively. Results are shown for normally incident waves with $a/h = 10$, $s = 0.6$ and $\lambda_n = 0.01$ for all n. We can see the two-dimensional model makes a good approximation for aspect ratios $b/a = O(10)$ with agreement improving for large values of Kb since this corresponds to a small incident wavelength relative to device width. Numerical efficiency was improved dramatically for wide rafts with computations performed for a raft made up of two equally-sized pontoons using the two-dimensional approximation being on average $O(10^3)$ faster than computations performed using the full model with $b/a = 8$.

Meanwhile, figure 4 shows the convergence of results computed using the full model of [9] to the slender-body approximation developed here. Results are shown for a system of two equally sized pontoons subject to normally incident waves with $b/h = 0.5$, $\hat{\lambda}_1 = 0.001$ and $s = 0.9$ fixed. Figures 4 (a), (b) and (c) correspond to $Kb = 0.4, 0.2$ and 0.1 respectively. Agreement between the full model and the slender body approximation is very good for $Kb = O(10^{-1})$, especially so for large Ka, corresponding to a large aspect ratio a/b.

For a narrow raft, Kb small, then the computational expense is marked since the decay of the infinite integrals defining inverse Fourier transforms in the y-direction is $O((Kb)^{-1})$. This results in increasingly large truncation sizes being required to evaluate the integrals numerically to an appropriate degree of accuracy. Since this narrow raft regime is of interest, applying to devices such as the Pelamis in real sea states, then more efficient computations are highly desirable. The speed of computations performed using the narrow raft approximation was on average $O(10^2)$ faster than those performed using the full model, a considerable improvement.

11

4. Continuously-damped plate model

In this section we are concerned with developing a simpler configuration which accurately models a floating raft made up of multiple pontoons. Thus, we consider an approximation in which the discrete raft sections are replaced by a continuously-damped plate model and the discrete power take-off applied in the hinges is replaced by continuous damping of the energy along the length of the device. The $N + 1$ equations of motion for the raft are thus reduced to a single kinematic boundary condition on the underside of the plate which incorporates its full dynamics. The velocity potential $\Phi(x, y, z, t)$ satisfies the hydrodynamic problem stated in [9, (2.3-2.6)]. Replacing the vertical displacements of the hinges and end-points, denoted by $\zeta_n(t)$, with the continuously varying vertical displacement of the raft, which will be denoted by $\zeta(x, t)$, the kinematic condition then becomes

$$\Phi_z(x, y, 0, t) = \dot{\zeta}(x, t) \qquad \text{for } (x, y) \in \mathcal{D}. \tag{4.1}$$

Further, factoring out harmonic time-dependence by writing

$$\dot{\zeta}(x, t) = \Re\left\{ \left(\frac{-iAg}{\omega} \right) \eta(x) e^{-i\omega t} \right\} \quad \text{and} \quad \Phi(x, y, z, t) = \Re\left\{ \left(\frac{-iAg}{\omega} \right) \phi(x, y, z) e^{-i\omega t} \right\}, \tag{4.2}$$

we find that $\phi(x, y, z)$ satisfies

$$\frac{\partial \phi}{\partial z}(x, y, 0) = \begin{cases} \eta(x) & \text{for } (x, y) \in \mathcal{D} \\ K\phi(x, y, 0) & \text{for } (x, y) \notin \mathcal{D} \end{cases} \tag{4.3}$$

along with [9, (2.8 and 2.9)], the remaining boundary conditions and governing equation defining the hydrodynamic problem remaining unchanged from the discrete model. The solution to this hydrodynamic problem will be considered in §4.2, but first we turn our attention to a continuous description of the raft's motion.

4.1. Kinematic boundary condition

In order to a kinematic boundary condition describing the raft's continuous motion we must first consider a discrete system of equations of motion for the raft expressed in terms of the vertical and rotational motions of the individual pontoons. This description of the raft's motion is largely guided by ideas used in [6] for a two-dimensional articulated raft. The equations describing the motion of the flexible raft may then be derived by taking the limit $a_n = \delta x \to 0$ whilst $N \to \infty$ so that a, and thus the dimension of the raft, remains constant. This derivation for the continuous equation is very similar to that of the Euler-Bernoulli beam equation in elasticity, see for example [5].

We begin by considering the vertical motions of the articulated raft. The interaction between adjacent pontoons is captured through R_n which denotes the vertical force exerted by pontoon n on pontoon $n + 1$. Applying Newton's second law for vertical motion we find

$$-i\omega M_n \left(\frac{\eta_n + \eta_{n-1}}{2} \right) = R_{n-1} - R_n + F_{w,n} - \frac{i}{\omega} C_n^v \left(\frac{\eta_n + \eta_{n-1}}{2} \right) \qquad \text{for } n = 1, ..., N \tag{4.4}$$

where the vertical wave force on the nth pontoon is given by

$$F_{w,n} = i\omega\rho \iint_{\mathcal{D}_n} \phi(x, y, 0) \, dx \, dy, \tag{4.5}$$

whilst the coefficients of the vertical accelerations and displacements in the inertial and buoyancy forces respectively are the mass and the weight of water displaced per unit depth of submergence,

$$M_n = 2\rho_s a_n b h \qquad \text{and} \qquad C_n^v = 2\rho g a_n b. \tag{4.6}$$

When considering the continuous limit $a_n = \delta x \to 0$ the discrete parameters describing articulated motion instead gain a continuous functional dependence on x and so we write

$$R_n \to R(x) \qquad \text{and} \qquad \eta_n \to \eta(x) \qquad \text{as} \qquad a_n \to 0 \tag{4.7}$$

12

where $R(x)$ now represents the continuous shear force and $\eta(x)$ is the continuous vertical velocity of the mat. Dividing (4.4) by a_n and taking limits results in

$$-2i\omega\rho_s hb\eta(x) = -R'(x) + i\omega\rho \int_{-b}^{b} \phi(x,y,0)\,dy - \frac{2i\rho bg}{\omega}\eta(x) \qquad \text{as} \qquad a_n \to 0 \qquad (4.8)$$

for $(x,y) \in \mathcal{D}$.

Next, we consider rotational motions. Applying Newton's second law to the rotational motion of the nth pontoon about its mid-point gives

$$-i\omega I_n \Omega_n = -\frac{1}{2}\left(X_n - X_{n-1}\right)\left(R_n + R_{n-1}\right) + X_{w,n} + X_{e,n} - \frac{i}{\omega}C_n^r \Omega_n \qquad \text{for } n = 1,...,N \quad (4.9)$$

where $\Omega_n = (\eta_n - \eta_{n-1})/a_n$ is the angular velocity of the nth pontoon. The wave torque on the pontoon is given by

$$X_{w,n} = i\omega\rho \iint_{\mathcal{D}_n} \phi(x,y,0)\left(x - \frac{X_n + X_{n-1}}{2}\right) dx\,dy \qquad (4.10)$$

whilst the rotary inertia and buoyancy coefficients are

$$I_n = \frac{M_n a_n^2}{12} \qquad \text{and} \qquad C_n^r = \frac{C_n^v a_n^2}{12} \qquad (4.11)$$

respectively and the external mechanical torque due to the damping in the hinges is given by

$$X_{e,n} = \lambda_n\left(\Omega_{n+1} - \Omega_n\right) - \lambda_{n-1}\left(\Omega_n - \Omega_{n-1}\right). \qquad (4.12)$$

Here λ_n describes the damping in the hinges due to power take-off for $n = 1,...,N-1$. In the continuous limit the angular velocities describing the rotational motion of the pontoons are expressed in terms of the continuous vertical velocity of the raft as

$$\Omega_n = \frac{\eta_n - \eta_{n-1}}{a_n} \to \eta'(x) \qquad \text{as} \qquad a_n \to 0. \qquad (4.13)$$

We also define an analogue of the power take-off parameter, describing continous damping of the bending motion along the length of the mat,

$$\lambda_n \to \hat{\lambda}/a_n \qquad \text{as} \qquad a_n \to 0. \qquad (4.14)$$

Thus, the external mechanical torques become

$$X_{e,n} = \lambda_n\left(\Omega_{n+1} - \Omega_n\right) - \lambda_{n-1}\left(\Omega_n - \Omega_{n-1}\right)$$
$$\to \hat{\lambda}\eta'''(x)a_n \qquad \text{as} \qquad a_n \to 0. \qquad (4.15)$$

Combining these equations, differentiating with respect to x, dividing through by a_n and taking limits we find

$$\frac{-2i\omega\rho_s bh^3}{12}\eta''(x) = -R'(x) + \hat{\lambda}\eta''''(x) \qquad \text{as} \qquad a_n \to 0 \qquad (4.16)$$

for $(x,y) \in \mathcal{D}$, the contributions due to wave and buoyancy torques having vanished in the limit.

Eliminating $R'(x)$ between these equations and dividing by $2i\rho bg/\omega$ we then gain the single equation

$$-ia^4\mathbb{B}\eta''''(x) + \mathbb{I}\eta''(x) + (1-\gamma)\eta(x) - \frac{K}{2b}\int_{-b}^{b}\phi(x,y,0)\,dy = 0 \qquad \text{for } (x,y) \in \mathcal{D} \qquad (4.17)$$

where

$$\mathbb{B} = \frac{\omega\hat{\lambda}}{2a^4\rho bg}, \qquad \gamma = \frac{\omega^2\rho_s h}{\rho g} \qquad \text{and} \qquad \mathbb{I} = \frac{\omega^2\rho_s h^3}{12\rho g} = \frac{h^2\gamma}{12}. \qquad (4.18)$$

13

In addition to (4.18) there are also free edge conditions which must apply on $x = \pm a$. Firstly, the shear force vanishes at the end points,

$$R(\pm a) = 0 \tag{4.19}$$

this is inherited from the fact that $R_0 = R_N = 0$ in the discrete system of equations and specifies that there is no external force. Substituting from (4.16) then (4.19) becomes

$$-ia^4 \mathbb{B} \eta'''(x) + \mathbb{I} \eta'(x) = 0 \qquad \text{on } x = \pm a. \tag{4.20}$$

Secondly, the bending moment vanishes at $x = \pm a$,

$$\hat{\lambda} \eta''(x) = 0 \qquad \text{on } x = \pm a, \tag{4.21}$$

since there is no damping force due to power take-off at the end-points. To make progress later we assume we can replace the average pressure across the width of the plate in (4.17) by the point wise pressure,

$$\frac{1}{2b} \int_{-b}^{b} \phi(x, y, 0) \, dy = \phi(x, y, 0). \tag{4.22}$$

This is an acceptable assumption where the plate is slender and the pressure is approximately constant across its width, but it also turns out to work well for wide rafts where the solution is approximately two-dimensional. The resulting set of equations (4.17, 4.20 and 4.21) are equivalent to the conditions on a flexing ice sheet adopted by Balmforth and Craster in [1] without shear deformation, frictional damping or flexing in the widthways direction. Here, the damping is provided by the power take-off and is related to the bending stiffness B of an ice sheet through $B \equiv |B| e^{i\psi} = -ia^4 \rho g \mathbb{B}$. Here ψ is the phase of the bending stiffness with $\psi < 0$ corresponding to dissipation. Thus, $|B| = a^4 \rho g \mathbb{B}$ and $\psi = -\pi/2$, describing dissipative rather than elastic effects.

Due to our small draft assumption we may neglect $\mathbb{I}$. Thus, combining (4.17) with (4.3) with these simplifications, we write the complete surface condition as

$$\left(\frac{\partial}{\partial z} - K \right) \phi(x, y, 0) = \begin{cases} \gamma \eta(x) + ia^4 \mathbb{B} \eta''''(x) & \text{for } (x, y) \in \mathcal{D} \\ 0 & \text{for } (x, y) \notin \mathcal{D} \end{cases} \tag{4.23}$$

along with the edge conditions

$$\eta'''(x) = \eta''(x) = 0 \qquad \text{on } x = \pm a. \tag{4.24}$$

With the dynamics of the plate now fully described by the surface boundary condition we turn our attention to a solution of the hydrodynamic problem.

4.2. Hydrodynamic Problem

We define the Fourier transform to be

$$\overline{\phi}(\alpha, \beta, z) = \int_{-\infty}^{\infty} \int_{-\infty}^{\infty} \left(\phi(x, y, z) - \phi_I(x, y, z) \right) e^{-i\alpha x} e^{-i\beta y} \, dx \, dy. \tag{4.25}$$

Then, taking Fourier transforms of the governing equations [9, (2.8 and 2.9)], it follows that

$$\left(\frac{d^2}{dz^2} - k^2 \right) \overline{\phi} = 0 \qquad \text{for } z < 0 \tag{4.26}$$

where $k = \sqrt{\alpha^2 + \beta^2}$ and $\overline{\phi} \to 0$ as $z \to -\infty$. Using (4.23) we also find that

$$\left(\frac{d}{dz} - K \right) \overline{\phi}(\alpha, \beta, 0) = \overline{I}(\alpha, \beta) \tag{4.27}$$

where

$$\overline{I}(\alpha, \beta) = \iint_{\mathcal{D}} \left(\frac{\partial}{\partial z} - K \right) \phi(x, y, 0) e^{-i\alpha x} e^{-i\beta y} \, dx \, dy \tag{4.28}$$

$$= \iint_{\mathcal{D}} \left(\gamma \eta(x) + i a^4 \mathbb{B} \eta''''(x) \right) e^{-i\alpha x} e^{-i\beta y} \, dx \, dy. \tag{4.29}$$

Thus, the Fourier transform solution is given by

$$\overline{\phi}(\alpha, \beta, z) = \frac{\overline{I}(\alpha, \beta)}{k - K} e^{kz}. \tag{4.30}$$

Invoking the inverse Fourier transform of (4.30) we gain an integral representation for $\phi(x, y, z)$

$$\phi(x, y, z) = \phi_I(x, y, z) + \frac{1}{4\pi^2} \int_{-\infty}^{\infty} \int_{-\infty}^{\infty} \frac{\overline{I}(\alpha, \beta)}{k - K} e^{i\alpha x} e^{i\beta y} e^{kz} \, d\alpha \, d\beta \tag{4.31}$$

and after differentiating with respect to z and setting $z = 0$ this results in an integral equation for $\eta(x)$

$$\eta(x) + (\mathcal{K}\eta)(x) = K e^{i\alpha_0 x} e^{i\beta_0 y} \tag{4.32}$$

where

$$(\mathcal{K}\eta)(x) = \frac{1}{4\pi^2} \int_{-\infty}^{\infty} \int_{-\infty}^{\infty} \frac{k}{K - k} \iint_{\mathcal{D}} \left(\gamma \eta(x') + i a^4 \mathbb{B} \eta''''(x') \right) e^{-i\alpha x'} e^{-i\beta y'} \, dx' \, dy' \, e^{i\alpha x} e^{i\beta y} \, d\alpha \, d\beta. \tag{4.33}$$

To solve (4.32) we expand the unknown vertical velocity $\eta(x)$, writing

$$\eta(x) \simeq \sum_{n=0}^{\infty} \frac{a_n w_n \left(\frac{x}{a} \right)}{a(\gamma + i\mathbb{B}k_n^4)}. \tag{4.34}$$

Here it is essential we choose $w_n(t)$ to be the eigenmodes of the Euler-Bernoulli beam equation

$$w_n''''(t) = k_n^4 w_n(t) \qquad \text{for } -1 < t < 1 \tag{4.35}$$

satisying free edge conditions

$$w_n'''(t) = w_n''(t) = 0 \qquad \text{for } t = \pm 1 \tag{4.36}$$

as required by (4.24). Substituting for this approximation in (4.32) the combination of η with η'''' reduces to a dependence on the function w_n alone since, using (4.35),

$$\gamma \eta(x) + i a^4 \mathbb{B} \eta''''(x) = \sum_{n=0}^{\infty} a_n w_n(x/a) / a. \tag{4.37}$$

The eigenvalue problem for $w_n(x)$ has the solutions

$$w_n(t) = \begin{cases} 1/2 & \text{if } n = 0 \\ it/2 & \text{if } n = 1 \\ \frac{1}{4} \left(\frac{\cosh(k_{2m}t)}{\cosh(k_{2m})} + \frac{\cos(k_{2m}t)}{\cos(k_{2m})} \right) & \text{if } n = 2m \\ \frac{i}{4} \left(\frac{\sinh(k_{2m+1}t)}{\sinh(k_{2m+1})} + \frac{\sin(k_{2m+1}t)}{\sin(k_{2m+1})} \right) & \text{if } n = 2m + 1 \end{cases} \tag{4.38}$$

resulting in a set of modes identical to that used by Newman in [8] for a similar problem. Meanwhile, the eigenvalues satisfy $k_0 = k_1 = 0$ along with

$$\tanh(k_{2n}) + \tan(k_{2n}) = 0 \qquad \text{and} \qquad \tanh(k_{2n+1}) - \tan(k_{2n+1}) = 0 \qquad \text{for } n > 1. \tag{4.39}$$

and the complete set of orthogonal eigenfunctions have the properties

$$\int_{-1}^{1} w_n(t) w_m^*(t) \, dt = \delta_{mn} c_m \qquad \text{and} \qquad \int_{-1}^{1} w_n(t) e^{-i\sigma t} \, dt = W_n(\sigma) \tag{4.40}$$

where the first two cases $(n = 0, 1)$ are given by

$$W_n(\sigma) = j_n(\sigma) \qquad \text{with} \qquad c_n = \begin{cases} 1/2 & \text{if } n = 0 \\ 1/6 & \text{if } n = 1 \end{cases}$$

whilst for $m > 0$

$$W_{2m+\nu}(\sigma) = \begin{cases} \sigma^2 \left(\sigma \sin \sigma + k_{2m} \cos \sigma \tanh(k_{2m}) \right) / \left(\sigma^4 - k_{2m}^4 \right) & \text{if } \nu = 0 \\ \sigma^2 \left(k_{2m+1} \sin \sigma \coth(k_{2m+1}) - \sigma \cos \sigma \right) / \left(\sigma^4 - k_{2m+1}^4 \right) & \text{if } \nu = 1. \end{cases} \tag{4.41}$$

with $c_{2m+\nu} = 1/8$ for $\nu = 0, 1$.

Substituting for the expansion of $\eta(x)$ given in (4.34) in the integral equation (4.32), multiplying through by $w_m^*(x/a)$ and integrating over $(x, y) \in \mathcal{D}$ results in the following system of linear equations for the unknown coefficients a_m,

$$\frac{a_m c_m}{(\gamma + i\mathbb{B} k_m^4)} + \sum_{n=0}^{\infty} a_n F_{mn} = KaW_m(\alpha_0 a) j_0(\beta_0 b) \qquad \text{for } m = 0, 1, 2, \ldots \tag{4.42}$$

where

$$F_{mn} = -\frac{ab}{2\pi^2} \int_{-\infty}^{\infty} \int_{-\infty}^{\infty} \frac{k}{k - K} j_0^2(\beta b) W_n(\alpha a) W_m(\alpha a) \, d\alpha \, d\beta \qquad \text{for } m, n = 0, 1, 2, \ldots. \tag{4.43}$$

Due to the symmetry properties of the W_n the integrals which determine F_{mn} vanish if $n + m$ is odd, a redundancy which allows us to decouple (4.42) into symmetric and antisymmetric parts,

$$\frac{a_{2m+\nu} c_{2m+\nu}}{(\gamma + i\mathbb{B} k_{2m+\nu}^4)} + \sum_{n=0}^{\infty} a_{2n+\nu} F_{2m+\nu,2n+\nu} = KaW_{2m+\nu}(\alpha_0 a) j_0(\beta_0 b) \tag{4.44}$$

for $m = 0, 1, 2, \ldots$ and $\nu = 0, 1$. Having developed a continuously-damped model of the raft we now consider an expression for the power.

4.3. Power

The power absorbed by a flexible raft is given by the time-averaged rate of working of the pressure force against the motion of the raft

$$W = \frac{\omega}{2\pi} \int_0^{2\pi/\omega} \left[\int_{-a}^{a} P(x, t) \dot{\zeta}(x, t) \, dx \right] dt \tag{4.45}$$

where the pressure force on the underside of the raft is given by

$$P(x, t) = -\rho \int_{-b}^{b} \Phi_t(x, y, 0, t) \, dy = \Re \left\{ \left(\frac{-iAg}{\omega} \right) \left(i\omega\rho \int_{-b}^{b} \phi(x, y, 0) \, dy \right) e^{-i\omega t} \right\}. \tag{4.46}$$

Thus, using a theorem on the averages of products, we find

$$W = \frac{1}{2} |Ag/\omega|^2 \Re \left\{ \int_{-a}^{a} \left(i\omega\rho \int_{-b}^{b} \phi(x, y, 0) \, dy \right)^* \eta(x) \, dx \right\}. \tag{4.47}$$

Substituting for the pressure force using the kinematic condition (4.23) results in

$$W = \frac{1}{2} |Ag/\omega|^2 \Re \left\{ \frac{2b\rho g}{\omega} \int_{-a}^{a} \left(a^4 \mathbb{B} \eta''''(x) + i(1 - \gamma)\eta(x) \right) \eta^*(x) \, dx \right\}. \tag{4.48}$$

16

Then, using the definition of $\mathbb{B}$ from (4.18) along with the fact that the second term is purely imaginary, this becomes

$$W = \frac{\hat{\lambda}}{2}|Ag/\omega|^2 \Re \left\{ \int_{-a}^{a} \eta''''(x)\eta^*(x)\,dx \right\}. \tag{4.49}$$

Further analytic simplification results after integrating by parts twice and using the edge conditions (4.24),

$$W = \frac{\hat{\lambda}}{2}|Ag/\omega|^2 \int_{-a}^{a} |\eta''(x)|^2\,dx \tag{4.50}$$

the power is thus given by the bending energy in the plate, $\eta''(x)$ being the curvature. It is worth noting that it is more convenient to use (4.49) since it involves fourth derivatives of the complex vertical velocity $\eta(x)$ allowing us to use (4.35) when substituting for the Galerkin expansion. In this way we ultimately gain

$$W = -\frac{\rho b g \mathbb{B}}{8a\omega}|Ag/\omega|^2 \sum_{n=2}^{\infty} \left| \frac{a_n k_n^2}{\gamma + i\mathbb{B}k_n^4} \right|^2 \tag{4.51}$$

where the sum starts at $n = 2$ since $k_0 = k_1 = 0$. This reflects the fact that the first two eigenmodes, being rigid plate modes, do not contribute to power.

4.4. Numerical Calculations and Results

For the purpose of numerical computation the infinite summation associated with the unknown vertical displacement of the plate is truncated at $n = 2N + 1$. All results in this section are shown for $a/d = 10$ and $s = 0.9$ along with the continuous damping parameter $\mathbb{B} = 0.01$ and the corresponding articulated power take-off parameters $\hat{\lambda}_n = N\mathbb{B}/8Ka$ for $n = 1, ..., N - 1$. In the continuously-damped model developed in this section we have made two approximations: (i) that the constituent pontoons are sufficiently short to approximate a continuously damped plate and (ii) that $\phi(x, y, 0)$ is constant across the width of the raft. In order to test the range of applicability of these two assumptions we consider the convergence of results computed using [9] to the continuously-damped model with increasing N and fixed length in the case of both wide and narrow rafts ($a/b = 4$ and 0.25 respectively). Results are presented in terms of the capture factor which, using an incident wave power $W_{inc} = \rho g |A|^2 \omega / 4K$, is given by

$$\hat{l} = \frac{W}{2bW_{inc}} = -\frac{1}{4Ka} \sum_{n=2}^{2N+1} |a_n|^2 \frac{\mathbb{B}k_n^4}{|\gamma + i\mathbb{B}k_n^4|^2}. \tag{4.52}$$

Figure 5 shows convergence of results computed using the full articulated model of [9] to the continuously-damped model with increasing N for $a/b = 4$ and 0.25. In both cases convergence is rapid, indeed articulated rafts results may barely be distinguished from the continuously-damped model with as few as 4 pontoons (just 3 hinges). Best agreement is seen for small values of Ka since this corresponds to long wavelengths relative to the device length, resulting in fewer bends in the continuous model and describing an articulated raft of relatively few sections. It is worth highlighting that we have made a narrow raft approximation in which the pointwise pressure across the width of the raft is assumed to be equal to the widthways average of the pressure. It is thus surprising that such good agreement is seen in the case of a modestly wide raft $a/b = 0.25$. The reasons for this are not fully understood. The case in which the raft is square (that is $a = b$) has also been tested and whilst the results are close to the continuous model, they converge to values that are not in such good agreement with the continuous model as those produced for modestly wide or narrow rafts. We conjecture that subject to normally incident waves the pointwise pressure across the majority of a wide raft is approximately equal to the average, the end effects being small and localised so that the dominant behaviour is well described by the model set out in §4.1.

We also consider variation in the vertical displacement of the raft along its length. Our interest in this is two-fold, firstly the formulation is based on a linearised theory of water waves
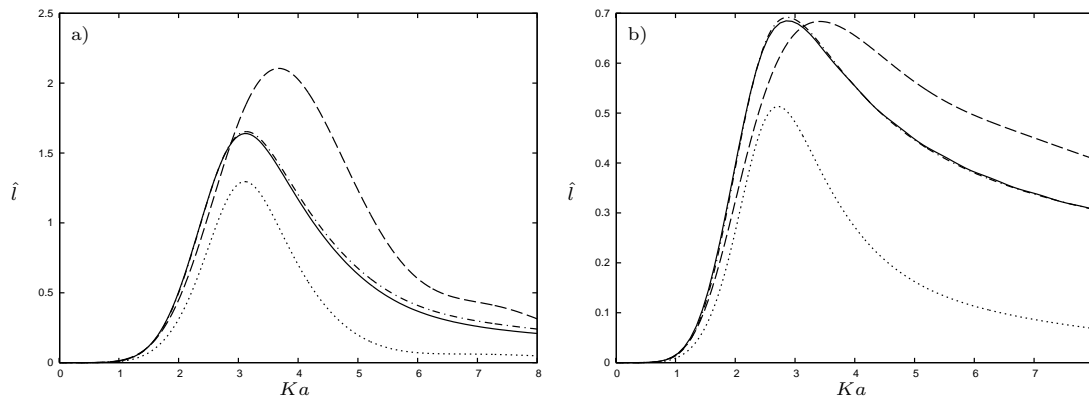
Figure 5: The figure shows a comparison of articulated raft results with the continuously-damped plate approximation with (a) and (b) plotting $\hat{l}$ as a function of Ka for $a/b = 4$ and $a/b = 0.25$ respectively. Dotted, dashed and chained curves represent systems of 2,3 and 4 pontoons whilst the solid lines show results corresponding to the continuously-damped plate model. In both cases $a/d = 10$ and $s = 0.9$ are fixed whilst power take-off is parameterised by $\mathbb{B} = 0.01$ and $\hat{\lambda}_n = N\mathbb{B}/8Ka$ for all n.

and there has been an *a priori* assumption that vertical excursions of the raft from its equilibrium position are small in order that results retain validity. We must therefore be careful to ensure that this assumption is justified in the results presented. Secondly, it allows us to inspect the maximum deformations of the raft and assess the importance of the number of pontoons at different dimensionless wave numbers.

The response amplitude operator (RAO) is used to characterise the motions of floating structures. In the case of the articulated raft the RAO is defined as the maximum vertical displacement of the nth node per unit height of incident wave ($H = 2A$) and is given in terms of the generalised modes of motion as

$$\left| \frac{\zeta_n(t)}{H} \right| = \frac{|\eta_n|}{H\omega} = \left| \sum_{m=0}^{N} U_m f_m(X_n) \right| / H\omega. \tag{4.53}$$

Meanwhile, for the continuously-damped plate model the RAO is given by the maximum vertical displacement per unit height of incident wave and is now a continuous function

$$\left| \frac{\zeta(x,t)}{H} \right| = \frac{|\eta(x)|}{2K} \simeq \frac{1}{2Ka} \left| \sum_{n=0}^{2N+1} \frac{a_n w_n \left(\frac{x}{a} \right)}{\gamma + i\mathbb{B}k_n^4} \right|. \tag{4.54}$$

In Figure 6 we see the RAO for an articulated raft made up of 8 pontoons and results computed using the continuously-damped plate model plotted as a function of position for $Ka = 1, 3.1$ and 7 and $a/b = 4$ fixed. For small Ka there is little variation in the maximum vertical displacements since the wavelength is long compared to the device length and the entire raft oscillates with little articulation. Comparing with the results in 5(a) we see that this corresponds to strong agreement between the continuously damped model and articulated raft along with minimal power absorption since bending has a minimal effect and the power take-off mechanism is not strongly engaged. There is much larger variation in the RAO along the length of the device for $Ka = 3.1$ since this is near to the peak in capture factor and the bending motions are thus greater. Finally, for large Ka then the incident wavelength is short relative to the device length and has little effect beyond the front section of the raft. This corresponds to a deterioration in agreement as the positioning of the points of articulation has a greater significance when the wave field is rapidly varying along the length of the raft.

5. Conclusions

In this paper we have developed approximations to an articulated raft-type device appropriate to three particular parameter regimes in which direct numerical methods of [9] struggle. The
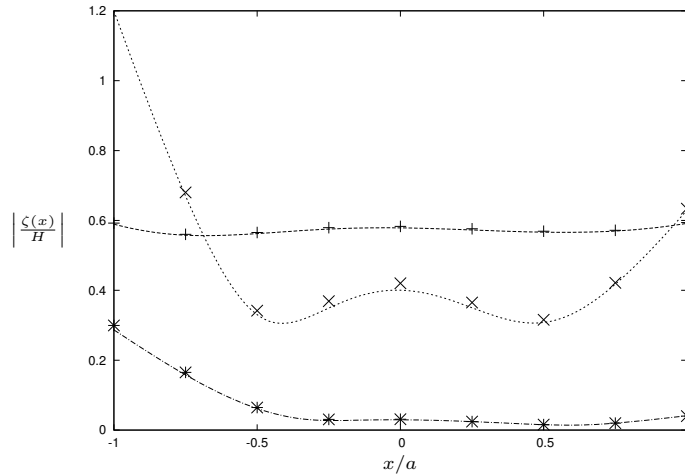
18

Figure 6: The figure shows a comparison of the articulated and continuously-damped raft motions, the RAO of the raft being plotted as a function of position for parameters corrersponding to figure 5(a). Dotted, dashed and chained curves correspond to the continuously-damped plate model with $Ka = 1, 3.1$ and 7 whilst crosses correspond to the discrete node displacements of an articulated raft made up of 8 pontoons.

include rafts with large aspect ratios (wide and narrow with respect to a reference angle of wave incidence) as well as a simplified continuum model for a raft with many articulations. In all cases, results have demonstrated good agreement in the key quantities determining the operation of the raft as a wave energy converter for parameters of physical interest. For example, 99% accuracy is obtained in capture width when either $Kb \geq O(10)$ (wide raft relative to the incident wavelength) or $Kb \leq O(1/10)$ (narrow raft relative to incident wavelength) whilst it has been shown that a continuum model of wave damping replicates the operation of rafts with 3 or more hinges within small margins of error. In each approximation the numerical effort required is reduced by orders of magnitude from full numerical simulations. This can be very important for design optimisation. It is possible these ideas could be applied to the operation of similar marine devices such as elongated anaconda, wave star or Kamei ship oscillating water column devices.

Acknowledgement

References

[1] Balmforth, N. and Craster, R. (1999). Ocean waves and ice sheets. *Journal of Fluid Mechanics*, 395:89–124.

[2] Barnett, A. (1996). The calculation of spherical bessel and coulomb functions. In *Computational Atomic Physics*, pages 181–202. Springer.

[3] Cockerell, C., Platts, M., and Comyns-Carr, R. (1978). The development of the wave-contouring raft. In *Wave energy conference. Abstracts of papers.*

[4] Gradshteyn, I. and Ryzhik, I. (1981). *Table of integrals, series and Products.* Academic Press, 111 Fifth Avenue, New York, New York 10003.

[5] Graff, K. F. (1975). *Wave motion in elastic solids.* Courier Corporation.

[6] Haren, P. and Mei, C. C. (1979). Wave power extraction by a train of rafts: hydrodynamic theory and optimum design. *Applied Ocean Research*, 1(3):147–157.

[7] Newman, J. (1979). Absorption of wave energy by elongated bodies. *Applied Ocean Research*, 1(4):189–196.

[8] Newman, J. (1997). Wave effects on hinged bodies. part i - body motions. Technical report, `http://www.wamit.com/publications.html`.

[9] Noad, I. and Porter, R. (2016). Modelling an articulated raft-type wave energy converter. *Submitted to Renewable Energy*. Available at: `https://people.maths.bris.ac.uk/~marp/abstracts/raft.html`.

[10] Porter, R. (2016). Surface wave interaction with rigid plates lying on water. *Wave Motion*.

[11] Thompson, I. and Porter, R. (2008). A new approximation method for scattering by long finite arrays. *The Quarterly Journal of Mechanics and Applied Mathematics*, 61(3):333–352.